SUPPORTING INFORMATION:

Two-Dimensional Multimode Terahertz Random Lasing with Metal Pillars

Yongquan Zeng[1], Guozhen Liang[1], Bo Qiang[1], Kedi Wu[1], Jing Tao[1], Xiaonan Hu[1], Lianhe Li[2], Alexander Giles Davies[2], Edmund Harold Linfield[2], Hou Kun Liang[3], Ying Zhang[3], Yidong Chong[4], and Qi Jie Wang[1,4,*]

[1]*Centre for OptoElectronics and Biophotonics, School of Electrical and Electronic Engineering, Nanyang Technological University, 50 Nanyang Avenue, Singapore 639798, Singapore*

[2] *School of Electronic and Electrical Engineering, University of Leeds, Leeds LS2 9JT, UK*

[3] *Singapore Institute of Manufacturing Technology, 2 Fusionopolis Way, Singapore 138634, Singapore*

[4] *School of Physical and Mathematical Sciences, Nanyang Technological University, 21 Nanyang Link, Singapore 637371, Singapore*

**Email: qjwang@ntu.edu.sg*

The supporting information includes:

1). Optical properties of individual dielectric and metal pillar structure.

2). Optical properties of different random dielectric pillar structures

3). The influence of emission apertures

4). Emission performance of different random metal pillar structures

1. Optical properties of individual dielectric and metal pillar structure.

In addition to the optical power spectra (Fig. 1a of the main text), the random structures with dielectric pillar and metal pillar are inspected over the modal properties respectively. For dielectric and metal structure, the pillar positions are the same. The structure comprises 680 scatterers, randomly distributed in a region of 500 μm × 500 μm. The dielectric pillar has a radius of 4μm and the area filling fraction (FF) of scatterers is 35%. While the radius of metal pillar is 4μm, leading to a FF of 13.6%. The scatterer position generation utilizes the same random placement algorithm method which imposes short-range order onto the disordered lattice and the scatterer size are optimized for dielectric pillar structure in the application of multimode localized random lasing around 3 THz range[1]. The optical power spectra and eigenmodes are calculated by 2D finite-difference time-domain (FDTD) simulations and 2D finite element method (FEM)

simulations, respectively. As the THz laser adopts subwavelength double metal structure in the vertical direction, the optical field in the vertical direction is uniform. Therefore, 2D simplified models to approximate 3D full-structure simulations. Eigenmodes have been scanned over different frequency ranges to provide sufficient resonant mode information.

Even though the simulation methods are different, the frequencies of the optical power spectra resonant peaks and eigenmodes have a good match. For disordered dielectric pillar lattice, it can be found that the optical power intensity is consistent with the eigenmode Q factor level in the whole interested frequency range (Fig. S1a). One obvious photonic gap can be found at ~ 3.5 THz and another gap is at ~ 6 THz (not visible mainly due to the weak short-range order). Tremendous optical intensity and Q factor drop can be found between the two sides of the photonic gaps. Strong resonant peaks with high Q are only found at the lower "bandedge" region, due to the fact that the lower "bandedge" modes are mainly overlapped with the dielectric pillars and higher "bandedge" modes are mainly located inside the lossy BCB. When the frequency goes away from the pseudo-gap frequency ranges, the Q factors drop quickly mainly due to the poorer in-plane modal confinement. In real devices, the free carrier loss of top/bottom contact layer and material loss of the gain medium (dielectric pillars in this case) have to be considered. Therefore, in 2D simulations, only the eigenmodes with Q > 200 are regarded as potential lasing modes. It can be found that the disordered dielectric pillar lattice can support random lasing in very limited frequency ranges (~ 2.85 – 3.4 THz and ~ 5 – 6 THz). The second frequency range is broader mainly due to the fact that the effective system size comparing to the wavelength is larger, which is advantageous for in-plane confinement.

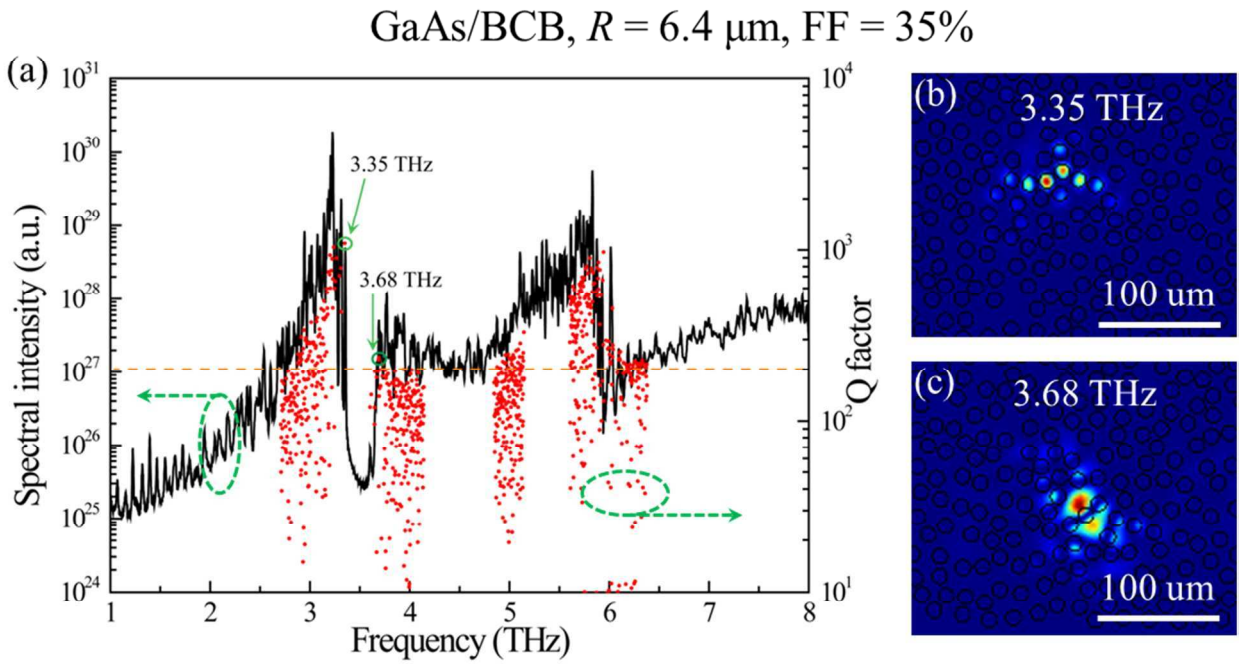

Figure S1. Optical power spectrum and eigenmode properties of a disordered dielectric pillar lattice (R = 6.4 μm, FF = 35%): (a) optical power spectrum (black curve) and calculated Q factors of the eigenmodes (red dots); typical field distributions at the (b) lower "bandedge" and (c) higher "bandedge" around the first pseudo-gap. The resonant peaks at 1-2 THz frequency range correspond to the low-Q Fabry-Perot resonances of the disordered lattice entity. Yellow dashed line outlines the Q factor of 200. The black empty circles correspond to dielectric pillars.

For disordered metal pillar lattice, numerous resonance peaks can be found in its optical power spectrum above 1.6 THz for a broad frequency range. These peaks are narrow (inset of Fig. S2), corresponding to high-Q resonant modes of the structure. Eigenmodes of the structure has been calculated. The typical eigenmodes are localized within the structure, similar to Fig. 2b in the main text. Even though the calculation has not been scanned over the whole frequency range, it can be inferred from Fig. S2 that the Q factor level gradually rises with increasing frequency. This can be explained by the larger effective structure size comparing to the wavelength. The highest Q factor is smaller than that of the dielectric counterpart. But it is worth to mention that the density of high-Q modes (Q > 200) which are promising to lase is much higher than that of the dielectric pillar structure (as shown by the statistical results in Fig. 3a and 3b in the main text). Most significantly, the high-Q mode frequency range is not limited, contrary to the case of disordered dielectric pillar lattice. This indicates that disordered metal pillar lattice is a more efficient random structure for broadband and multimode THz random lasing.

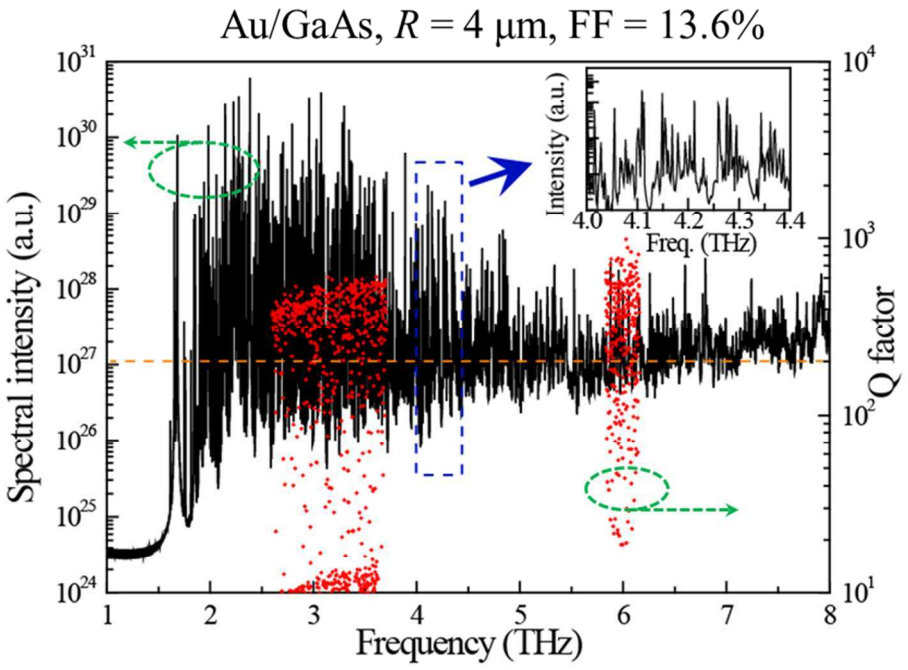

Figure S2. Optical power spectrum (black curve) and eigenmode properties (red dots) of a disordered metal pillar lattice (R = 4 μm, FF = 13.6%). Yellow dashed line outlines the Q factor of 200. Inset: the detailed optical power spectrum at 4.0 THz – 4.4 THz frequency range. Multiple narrow peaks can be observed.

2. Optical properties of different random dielectric pillar structures

In the above discussions, it seems unreasonable to compare disordered dielectric pillar lattice and disordered metal pillar lattice with different scatterer sizes. Here, it is necessary to emphasize that the disordered dielectric pillar structure has been optimized according to the Ref. 1 for better random lasing performance at ~ 3 THz.

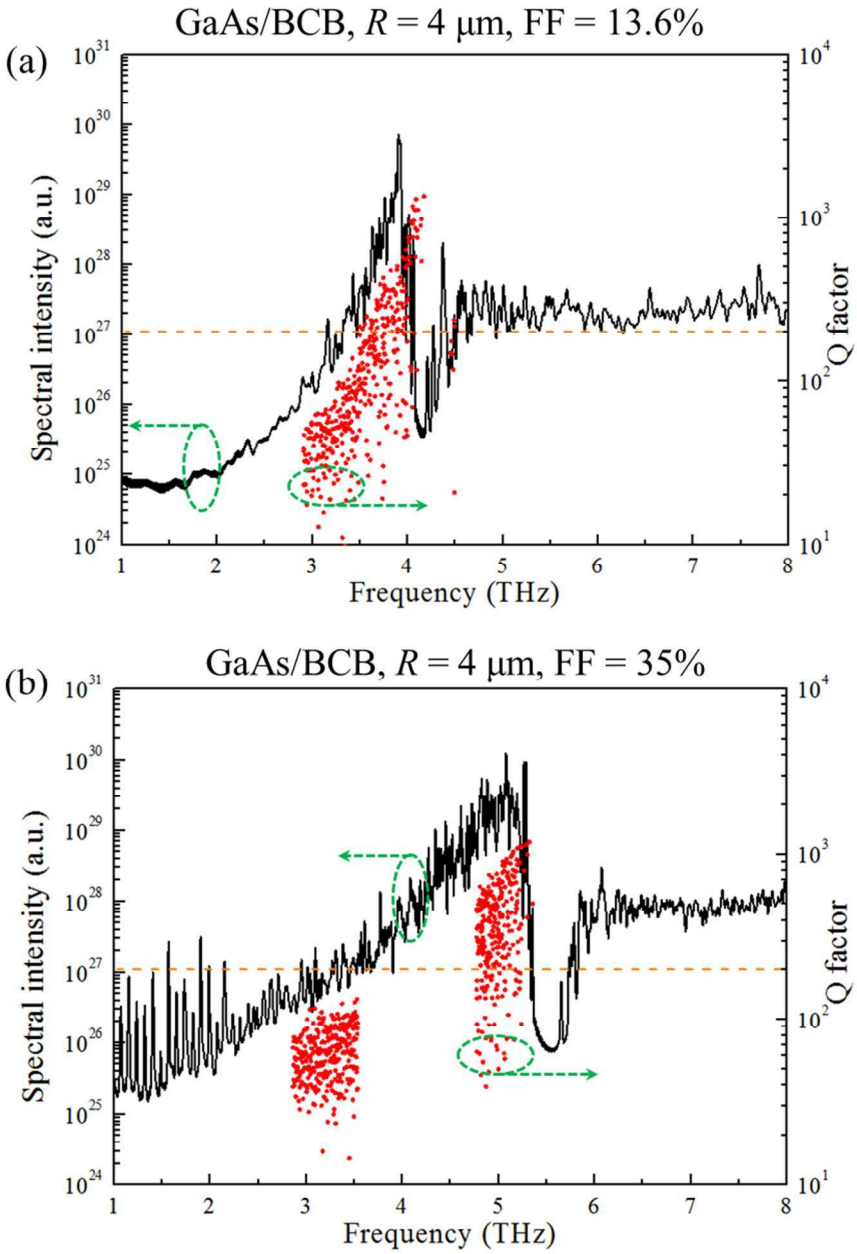

Figure S3. Optical power spectrum (black curve) and eigenmode properties (red dots) of disordered dielectric pillar lattices with (a) R = 4 μm, FF = 13.6% and (b) R = 4 μm, FF = 35%. Yellow dashed line outlines the Q factor of 200.

The optical properties of random dielectric pillar structure with different parameters have also been studied. As shown in Fig. S3a, the disordered dielectric pillar lattice with smaller scatterer size (R = 4 μm, scatterer positions keep the same as in section 1) supports high-Q resonant modes at ~ 3.9 THz, mainly due to the fact that the Mie resonances of dielectric pillars are tuned to higher frequency range with smaller pillar size. Only one weak pseudo-gap can be found in the spectrum with much less high resonant peaks. This indicates that the overall scattering strength of the random structure is weak. So it is reasonable to increase the FF of dielectric pillars. Fig. S3b shows the optical power spectrum of a random dielectric pillar structure with R = 4 μm and FF = 35%. The first pseudo-gap is shifted to even higher frequency range (~ 5.5 THz). This is induced by a smaller effective lattice period $a \propto r/\sqrt{FF}$ [1]. And the high-Q mode frequency range is larger than that of the Fig. S1 structure, again can be explained by the larger effective system size comparing to the wavelength. The second pseudo-gap is found at ~ 9.4 THz (not shown here).

To conclude, the parameters (R = 6.4 μm, FF = 35%) of disordered dielectric pillar lattice is optimized for random lasing at 3 THz frequency range which is the gain spectral range of the THz QCL wafer used in this work. Therefore, significance of this work can be uncovered by a comparison between the proposed random metal pillar structure and the optimized random structure with dielectric pillars which has the best performance reported so far at THz frequency range.

3. The influence of emission apertures

The influence of emission apertures on the optical modes has been investigated by 3D FEM simulations using Comsol Multiphysics. The metal pillars are randomly distributed in a region of ~ 190 μm × 190 μm with R = 4 μm, FF = 13%. The 2D random structure with 10μm height is sandwiched by top and bottom metal layers (as shown by Fig. 4 in the main text) which are advantageous for optical confinement in the vertical direction and simultaneously work as electrodes for current injection[2]. Multiple absorbing boundary layers are used to eliminate the boundary reflections. Thus, the calculated eigenmodes (black squares in Fig. S4) are completely supported by the disordered metal pillar lattice. For the random structure with emission apertures, 87 (FF = 5%) air holes with radii R = 2.5 μm are created in the top metal layer. The air holes and metal pillars are not overlapped. The active region material loss and ohmic loss of metal are not considered in the calculations.

It can be found from Fig. S4 that the eigenmode frequencies have a blue shift when emission apertures are considered in the simulations, mainly due to the fact that the tail of electromagnetic field extends into the air, leading to a smaller modal effective refractive index. With the geometry size of the cavity unchanged, a smaller effective refractive index means a shorter resonant wavelength. The blue shift varies for different eigenmodes, indicating the apertures impose different influences on the optical modes. The eigenmode Q factors are also influenced by the existence of emission apertures. Some of the eigenmodes have lower Q factors when there are

emission apertures since the photon can escape through these small air holes; while some other eigenmodes unexpectedly get enhanced Q factors (e.g. eigenmodes at ~ 3.11 THz) when the apertures are introduced. The larger Q factors may be due to better in-plane optical confinements contributed by the introduced emission apertures in certain special positions. The eigenmode field distributions for the random structure with and without emission apertures have been compared. As can be seen in Figure S5, the emission apertures exert small influence on the field distributions no matter how the eigenmode Q factors are influenced. The emission apertures cannot solely support high-Q modes as the aperture size is in deep subwavelength range. This indicates that the smaller air holes in the top metal layer mainly work as emission outcouplers.

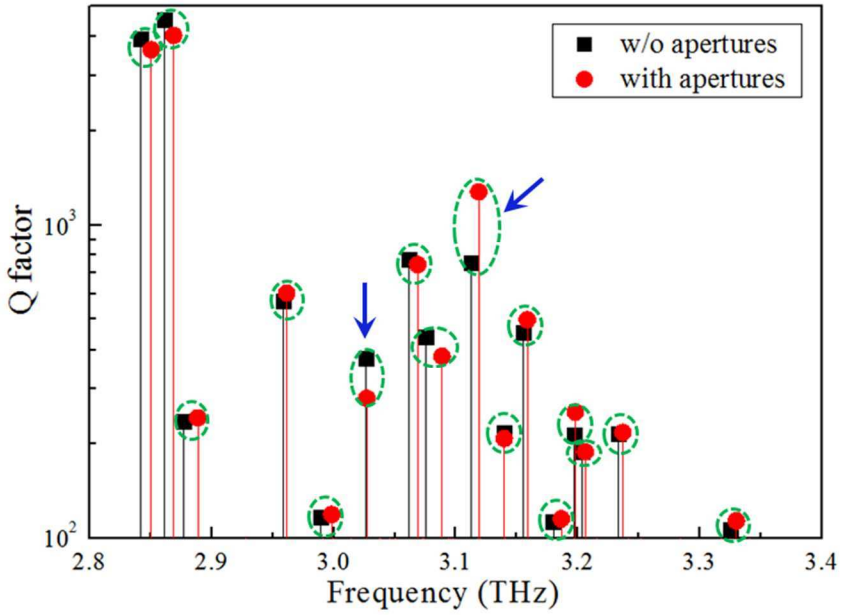

Figure S4. Eigenmode Q factors of a random metallic pillar structure with (red dots) and without (black squares) emission apertures. The two corresponding modes of the random structure with and without emission apertures are grouped by blue dashed circles. The field intensity distributions for the eigenmodes highlighted by blue arrows will be shown in Figure S5.

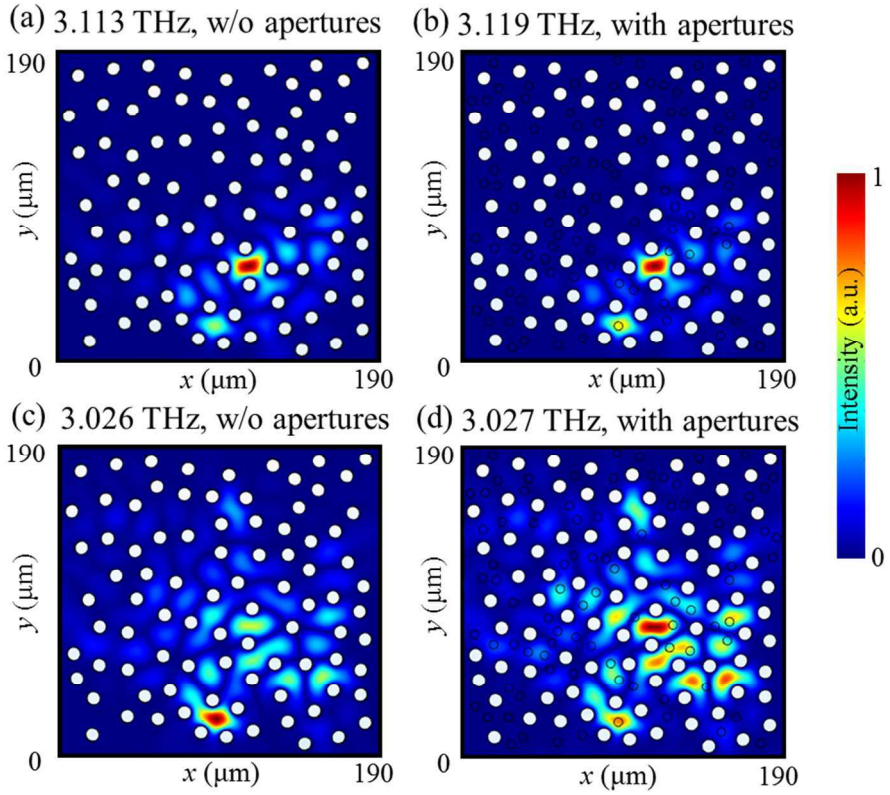

Figure S5. The two eigenmode field distributions for a random metallic pillar structure without emission apertures (a), (c) and the corresponding eigenmode field distributions for the random structure with emission apertures (b), (d). The white solid circles (R = 4 μm) correspond to randomly distributed metal pillars and the black empty circles (R = 2.5 μm) in (b), (d) are emission apertures.

The influence of aperture number on the random laser emission performances has also been studied experimentally. 3% FF of apertures was initially created in the top metal layer using FIB etching and the laser performance was characterized. Then the aperture FF was increased to 5% using the same method on the same device and the laser was characterized again. It is found that with more apertures, the peak frequencies have blue shifts. The frequency shift varies for different modes, similar to the simulation results in Fig. S4. Some emission peaks (black dashed arrows) get stronger indicating that these modes get more power extracted with slight influence on the modal Q factors. Some (blue dashed arrows) become weaker, indicating that additional apertures seriously reduce the modal Q factors. In addition, new emission peaks (green solid arrow) also appear. This indicates that the aperture number and positions are important for a lasing mode. But as the structure itself is random, the positions and number of apertures impose a random influence on the laser performances. It can be imagined that there would be an optimal combination of the aperture size, aperture filling fraction and position for a typical random metallic pillar structure which could achieve a better emission power, more emission modes with comparably low threshold. But this needs statistical full-structure 3D simulations and experimental verification, which is not practical due to the large parameter searching space.

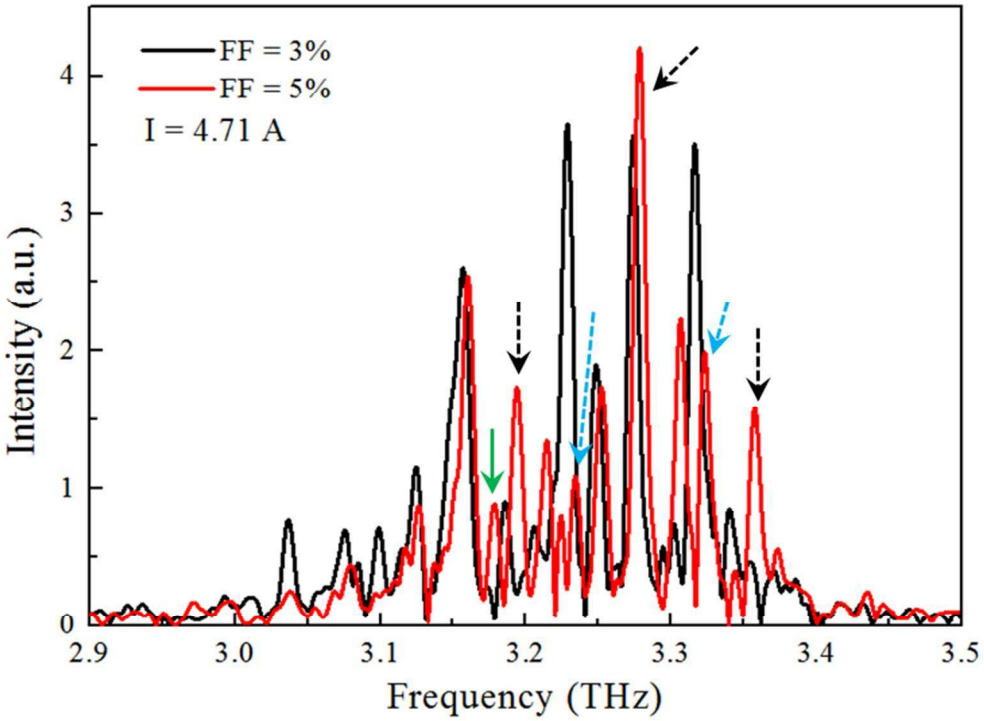

Figure S6. The emission spectra of the fabricated random laser with FF = 3% (black) and FF = 5% apertures (red). The radius of apertures is 2.5μm. The random metal pillar structure has a size of ~ 515 μm × 515 μm with R = 4 μm, FF = 11%. With more apertures, some emission peaks get stronger (black dashed arrows); some peaks (blue dashed arrows) become weaker; and new emission peaks (green solid arrow) also appear.

4. Emission performance of different random metal pillar structures

Random metallic structures with different filling fractions have been fabricated and characterized. The device characterization method is detailed in the main text. Due to the fact that the gain spectral range of THz quantum cascade laser (QCL) wafer has a blue shift with increasing pumping current, the emission spectra of each device are intentionally selected to fully present all the identified random lasing peaks. As shown in the Fig. S7, the random lasers with FF = 10%, 11%, and 13% also have complex emission spectra and the emission mode number are more than 20, comparable to the results presented in the main text. The structures with FF = 16% and FF = 17% have less emission modes, since there are simultaneous smaller gain volume (the material gain was not considered in the theoretical calculations in the main text) and larger metal free carrier loss for higher FF structures. The emission apertures are randomly distributed and the positions are not optimized, which is also a possible reason for less emission modes. Overall, the experimental results are consistent with the theoretical analysis.

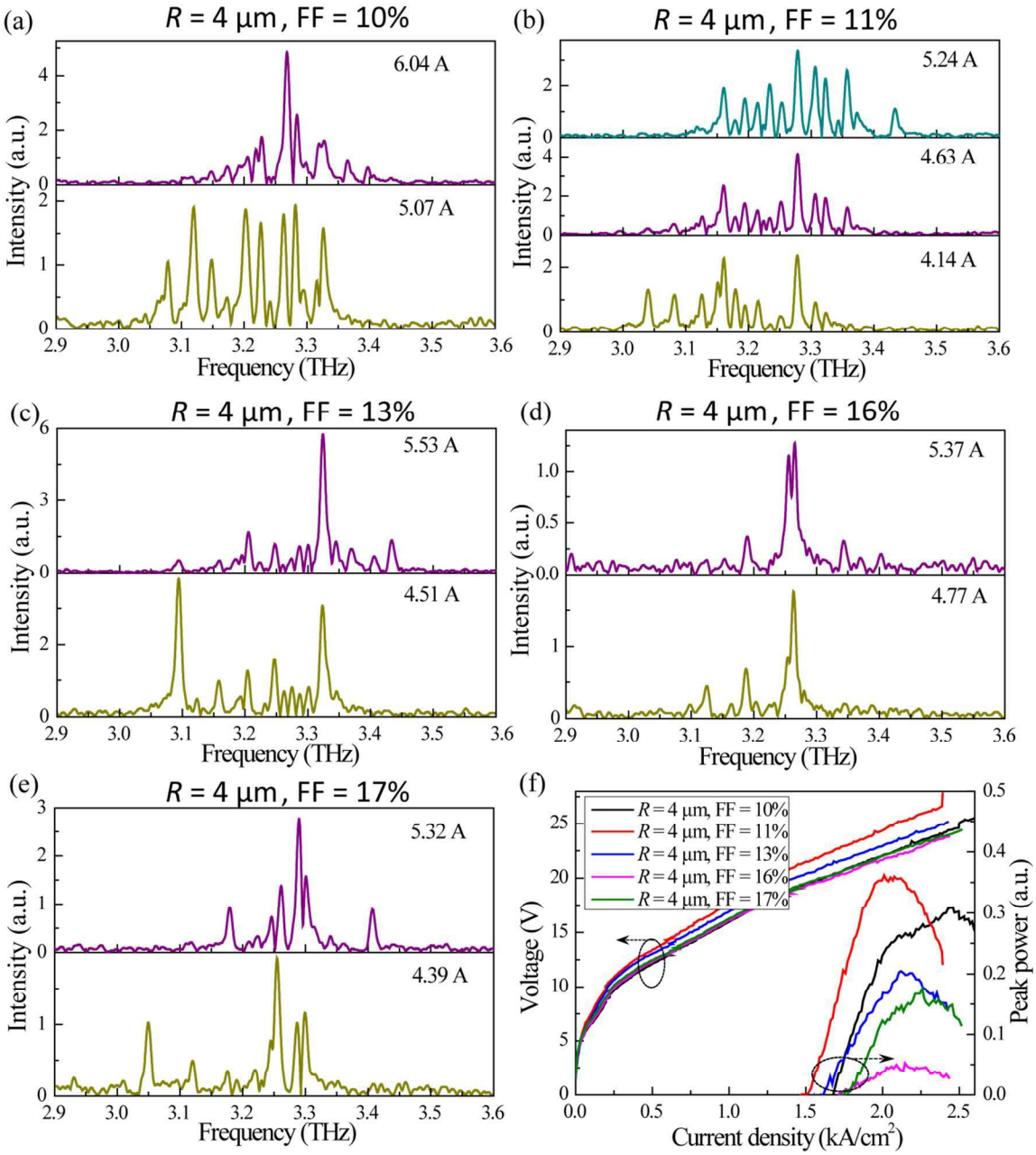

Figure S7. (a)–(e) Emission spectra of different random metal pillar structures and (f) light-current-voltage (LIV) curves. All the emission spectra are measured at 9 K with the corresponding pumping current indicated in the figures. The laser with area of ~ 515 μm × 515 μm is operated in pulsed mode with a repetition rate of 10 kHz and a pulse width of 500 ns.

References

(1) Zeng, Y.; Liang, G.; Liang, H. K.; Mansha, S.; Meng, B.; Liu, T.; Hu, X.; Tao, J.; Li, L.; Davies, A. G.; Linfield, E. H.; Zhang, Y.; Chong, Y.; Wang, Q. J. Designer Multimode Localized Random Lasing in Amorphous Lattices at Terahertz Frequencies. *ACS Photonics* **2016**, *3*, 2453–2460.

(2) Unterrainer, K.; Colombelli, R.; Gmachl, C.; Capasso, F.; Hwang, H. Y.; Sergent, A. M.; Sivco, D. L.; Cho, A. Y. Quantum Cascade Lasers with Double Metal-Semiconductor Waveguide Resonators. *Appl. Phys. Lett.* **2002**, *80*, 3060–3062.